Proceedings of ASME Turbo Expo 2017
GT2017
June 26-30, 2017, Charlotte, USA

GT2017-63788

COMPUTATIONAL AND EXPERIMENTAL STUDY OF A PLATINUM THIN-FILM BASED OIL CONDITION AND CONTAMINATION SENSOR

V. Sridhar and K. S. Chana
Osney Thermo Fluids Research Laboratory
Department of Engineering Science
University of Oxford
Oxford, United Kingdom

D. Singh
Department of Mechanical Engineering
Indian Institute of Technology Delhi
New Delhi, India

ABSTRACT

Lubrication systems form an integral part of aircraft and automobiles. Failure of lubrication systems can occur due to contamination or degradation of oil which can be quite disastrous, especially for an aircraft. This will also lead to unnecessary downtime and increase in maintenance cost. Oil contamination occurs when metallic or non-metallic particles are produced due to wear of machine components such as bearings, gears etc. and these particles may not be always captured by the filtering system that are already in the lubrication system. Due to this, the particles can clog oil paths and accelerate the wear of moving parts. In addition to this, variations in thermal stresses causes oxidation and thereby degradation of the oil. Contamination can also be in the form of liquids such as water droplets or fuel from heat exchangers. Currently, on-line oil condition monitoring systems use sensors that are based on eddy current, optical, capacitive to detect contamination in oil for preventive maintenance especially for aircraft engine bearings, aviation gearboxes etc. These sensors have some major drawbacks: prone to surface contamination, non-linearity, insensitive to detect extremely small particulates or false detection such as trapped bubbles.

A new sensor based on platinum thin film heat transfer gauges has been developed at the University of Oxford that works on the principle of measuring the change in thermal product of the material that is in contact with the sensor. The sensor is able to detect any form of contamination in oil and can be used for both off-line and on-line condition monitoring. The sensor is found to be quite sensitive and can detect extremely small concentrations of contaminants of the order 0.01 percent by mass. This paper presents a detailed computational and experimental study carried out to test various forms of contamination in oil. The three-dimensional, time-dependent, implicit numerical simulations were carried out using the commercial computational fluid dynamics package FLUENT. The simulation incorporates conjugate heat transfer to obtain the heating curves of the sensor with and without contamination. This was necessary to understand the range of the sensor and also to study the variations in heat transfer from the sensor to the material that is in contact with the sensor, which otherwise could not have been possible through experiments. The numerical heating curves are then compared with experimentally obtained heating curves and the comparison showed that the numerical and experimental data seemed to agree quite well and were within 1 percent.

INTRODUCTION

Development of sensors for oil contamination and condition monitoring is an active area of research in Aerospace and Mechanical industry. Currently available sensors to measure oil contamination are becoming an established method to predict and avoid breakdowns of gas turbine engines, automotive engines, manufacturing machines etc. Most of the oil condition monitoring is carried out in real-time such as your “change oil” sensor in an automobile or other machinery. The monitoring can also be performed offline in a laboratory, although this can be quite time consuming. Some of the real time sensors currently

used are eddy current, capacitance, Hall effect etc. These sensors work well in detecting contamination, however, they are temperature dependent and insensitive to extremely small concentrations of the contaminant. Optical based contamination detection techniques, such as infrared spectrometry have a limitation of contamination of optics and also can be quite expensive. Eddy current and Hall effect sensors can detect only metallic particles [1]. Acoustic sensors have also been developed to measure the changes in viscosity using micro acoustics [2] or by measuring the shear motion of a piezoelectric resonator immersed in oil [3]. However, these are temperature dependent and are prone to false readings.

A new sensor based on platinum thin film heat transfer gauges has been developed at the University of Oxford that works on the principle of measuring the change in thermal product of the material that is in contact with the sensor and its application in the detection of contamination in oil, fuel etc. for real-time applications. We present some numerical and experimental studies carried out on the sensor with liquid contamination to understand the heat transfer process in order to improve the sensor.

WORKING PRINCIPLE AND THEORY

As mentioned in the previous section, the sensor can detect the change in thermal product of the material that is in contact with the sensor. An electrical square pulse of certain amplitude and duration is passed through the sensor and the sensor's temperature increases as some of the heat is dissipated in the sensor's bottom and some is dissipated in the surrounding material and a certain temperature is recorded by the sensor. As the surrounding material composition changes, the dissipated heat between the sensor substrate and surrounding material changes. The change can be correlated to the change in thermal product of the material. In the case of contamination of oil, the thermal product will be different for the contaminants compared to the oil (Thermal product $\sqrt{\rho ck}$ for oil is 500 and metals is 22,000) and hence the heat transfer will be different [4].

The relation between heat transfer and thermal product is derived as follows:

The one dimensional unsteady heat transfer equation is given as

$$\frac{\partial^2 T(x,t)}{\partial x^2} = \frac{1}{\alpha(x)} \frac{\partial T(x,t)}{\partial t} \tag{1}$$

where T is temperature, x is distance in the substrate, t is time and

$$\alpha = \frac{\rho}{kc} \tag{2}$$

TABLE 1: Thermal properties of the liquids

Material	Density ρ (kg/m^3)	Heat capacity c_p (J/kgK)	Thermal conductivity k (W/mK)	Thermal product J/m^2Ks^2
Water	998.2	4182	0.6	1582
Acetone	791	2160	0.18	555
Oil	884	1910	0.14	486

The analytical solution for a step function in temperature (see [5]) of this equation is evaluated as:

$$\dot{q}_{wall} = (T_{wall} - T_0) \frac{\sqrt{\pi}}{2} \frac{\sqrt{\rho ck}}{\sqrt{t}} \tag{3}$$

where $\dot{q}_{wall}$ is heat transfer rate, T_{wall} is wall temperature, T_0 initial conditions.

$$q_{wall} \propto \sqrt{\rho ck} \tag{4}$$

This shows that the heat transfer to a material is directly proportional to the thermal product of that material.

Table 1 gives the thermal properties and thermal product values for water, acetone and oil. We note that the thermal product values are quite different and the sensor should be able to detect these changes.

Numerical Setup

Three dimensional computational fluid dynamic simulations were carried out on the sensor along with the oil pot to study the conjugate heat transfer between the thin film gauges and the surrounding fluid. Figure 1a shows the CAD model of the oil pot and the sensor that was created with SOLIDWORKS®. Contamination in the liquid was modelled using hemispherical volumes placed on the sensor as shown in Fig. 1b . The size of the bubble was increased as the level of contamination increases. The geometry was then imported in ANSYS Design Modeler®to specify various boundaries and surfaces. ANSYS workbench®meshing was used to create an unstructured mesh as shown in Fig. 2 with tetrahedral elements. To study the conjugate heat transfer, nodes at solid-fluid interface were matched using proper face sizing and inflation. ANSYS FLUENT®was used to carry out the CFD simulations. The transient pressure-based solver was used to solve the Navier-Stokes and the energy equation. Time was discretized using the second order implicit scheme. For pressure-velocity coupling, SIMPLE scheme was used and the green-gauss node based method was used for spatial

discretization, as it is more accurate and best suited for tetrahedral meshes. Second order upwind schemes were used to solve for pressure, momentum and energy. The solution was initialized with pressure and velocities set to zero and an initial temperature of 300 K. The platinum thin film gauge acted as a constant source of heat input ($7.143\,\mathrm{GW/m^3}$) for a 5 ms pulse duration. A time step of 0.5 ms was used with each time-step having a maximum of 20 iterations to achieve the convergence.

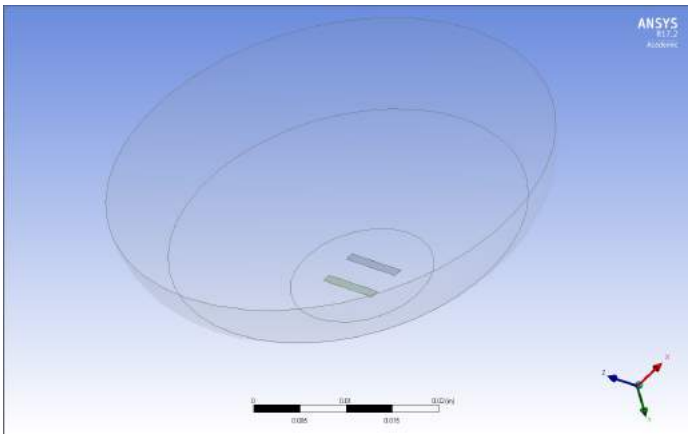

(a) Control volume

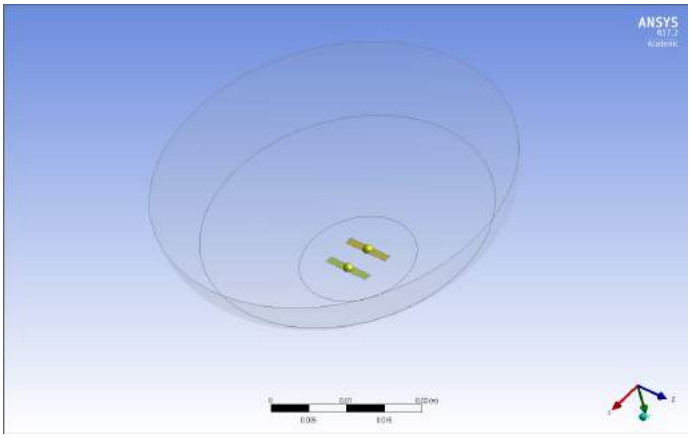

(b) Control volume with contamination

FIGURE 1: 3-D model of the control volume

Grid Convergence Study

A grid convergence study was performed for both cases i.e with and without contamination before performing the full set of numerical simulations. Three grids were selected that are labelled as coarse, medium and fine. The grid size for each case is given in table 1.

Mesh	Without Contamination	With Contamination
Coarse	471593	516154
Medium	1317412	1351388
Fine	4584290	4589542

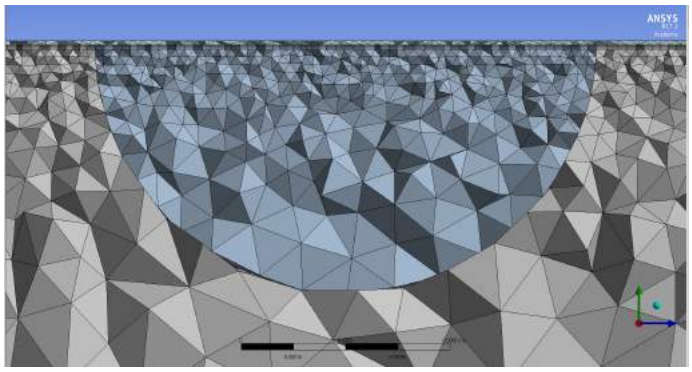

FIGURE 2: Grid with contamination

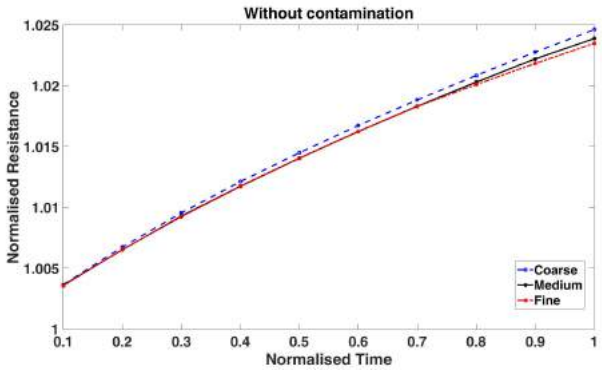

(a) Without contamination

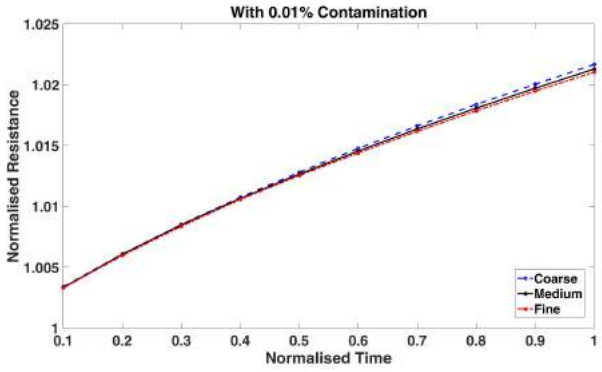

(b) With contamination

FIGURE 3: Grid convergence study

Figure 2 shows a typical grid with contamination. The contamination is modelled as a hemispherical volume in the liquid placed on top of the sensor as mentioned in the previous section. For grid independence study with contamination we chose the contamination to be 0.01 %. Figures 3a and 3b show the the thermal product curves (normalised resistance values) for the three grids without and with contamination. We clearly note that the curves collapse quite well for all three grids and the variation between the medium and fine mesh is significantly small. We decided to use the "medium" mesh for all the cases without and with contamination. For the case with contamination, the grid size varies based on the concentration of the contamination which means a varying bubble size. However, the number of grid points on the sensor and the first cell height, expansion ratios were kept constant.

Experimental Setup

Experiments were carried out to validate the numerical simulations. The experiments comprised of an oil pot as shown in Fig. 4a with a sensor at the bottom. The sensor had two thin film gauges made of platinum and these gauges were painted on a MACOR® substrate. The fluids used in the experiments were oil, acetone and water. A micro-litre syringe was used to supply the contamination at the required concentrations with the lowest concentration being 2 μL corresponding to 0.01% by mass for 20 mL of fluid. The electronic device to send the electrical pulse and measure the response was made by Proxisense®(Fig. 4a). The device consists of a 24-bit Analog to Digital Converter sampling at 4.8 kHz and can be configured to have varying pulse amplitude, width and frequency. In the tests carried out, the pulse amplitude was fixed at 5 V, the width was 5 ms and the frequency of pulsing was 2 s. The data from the device was acquired and then analysed using MATLAB®.

Without Contamination

Numerical simulations were carried out to check the suitability of the chosen numerical model for the present application by comparing with the experimental data. The tests comprised of testing water, acetone and oil individually. From Fig. 5, we see that the numerical results agree quite well with the experimental data. Both numerical simulations and experiments show that, as the thermal product (see table 1) increases, the curve shifts downwards, which is expected as the amount of heat absorbed is more with materials with high thermal products. We also note that simulations were able to capture the slight difference in thermal product between acetone and oil.

Table 2 shows the comparison of the final value of the thermal product curves with experiments. The percentage difference is calculated using equation 5. The variations between the simulations and experiments are found to be within 1 percent which

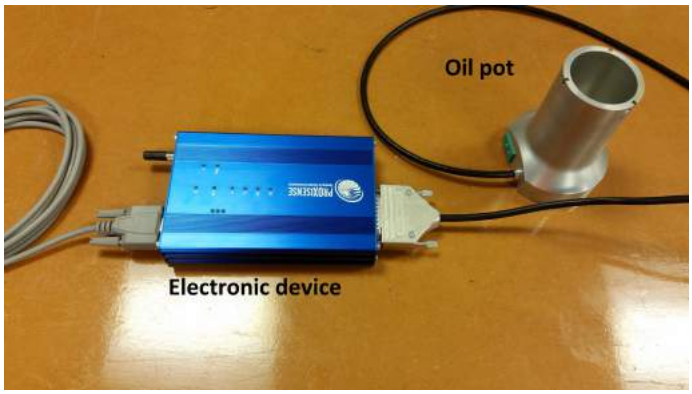

(a) Experimental setup

(b) Thin film gauge sensor

FIGURE 4: Experimental setup and the sensor

is quite good. However, it should be pointed that there is large variation for the initial part of the curves especially for acetone and oil between simulations and experiments.

$$\%\text{Difference} = \frac{\text{NR}_\text{C} - \text{NR}_\text{E}}{\text{NR}_\text{E}} * 100 \tag{5}$$

The penetration depths for water, acetone and oil is given in Fig. 6. Penetration depth is quite important to set the sensitivity of the sensor in experiments. Longer the pulse width and amplitude, higher will be the penetration. This will enable the sensor to detect large concentrations of contamination. The penetration depth is obtained by looking at the temperature variation along a vertical line in the z-direction drawn from the mid-point of one of the sensors to the end of the top domain. From Fig. 6, we note that the temperature for all three liquids approximately reaches

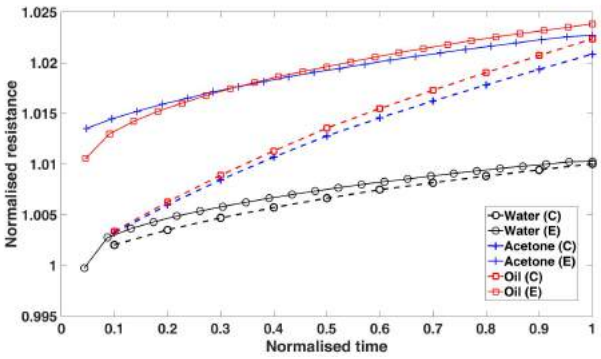

FIGURE 5: Comparison between CFD and Experimental data without contamination

Material	Computation	Experiment	% Difference
Water	1.01	1.0103	0.0297
Acetone	1.021	1.023	0.1955
Oil	1.022	1.024	0.1953

TABLE 2: Comparison of final values of thermal product (resistance) between computations and experiments

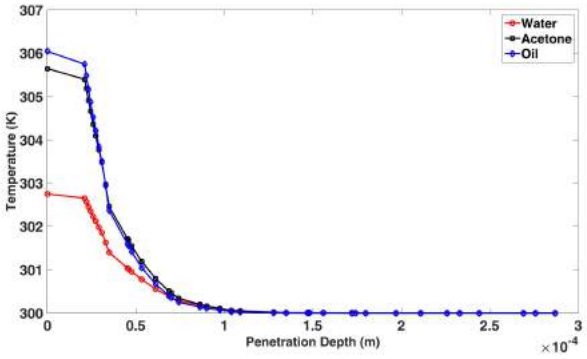

FIGURE 6: Penetration depth

the initial temperature of 300 K at $\approx$ 0.15 mm

With Contamination

In the previous section, we see that we get good agreement with the CFD and experimental data for the three cases investigated. Here, numerical simulations are carried out with contamination of varying concentrations and compare it with the experimental data. We look at two types of liquid contamination: Water in acetone and Water in oil with varying concentrations from 0.01% to 1%. The former case is a general study to see how the numerical model compares with the experiments. However, this can be related closely to fuel contamination. The latter case is what is generally found in gas turbine engines and other machinery where the moisture gets trapped in the oil.

Water in acetone and oil

Figures 7 and 8 show the contour plots of static temperature for 0.01% and 1% concentrations of water in acetone and oil at the end of the pulse (i.e. 5 ms). We note that as the concentration increases, more heat is absorbed by the water due to its high thermal product compared to the acetone. Due to this heat transfer phenomenon of more heat being absorbed by water from the sensor, the temperature where the water bubble is located is much lower compared to the rest.

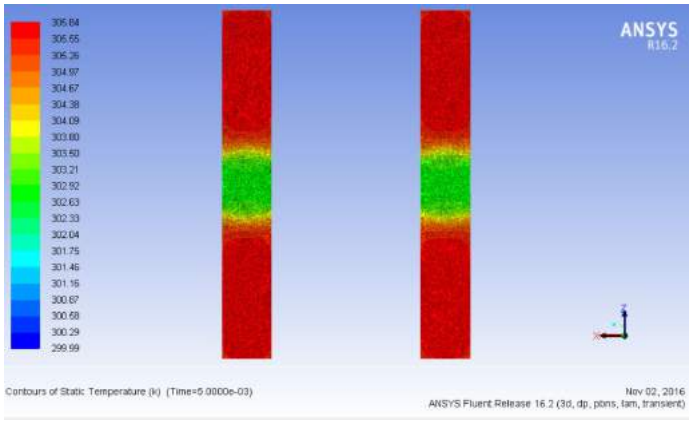

(a) 0.01% of water in acetone

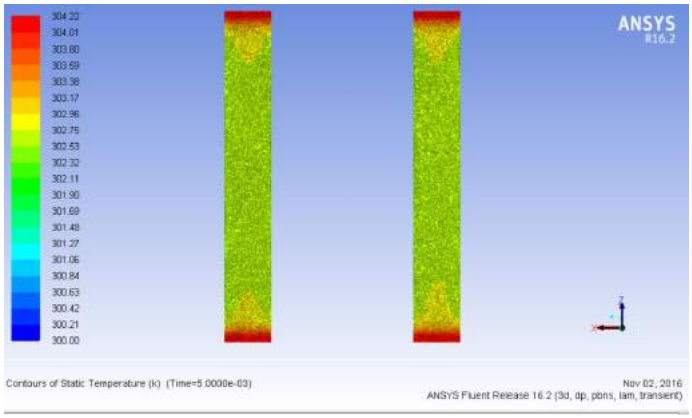

(b) 1% of water in acetone

FIGURE 7: Contour plots of Temperature for water in acetone

Figures 9a and 9b show the comparison of thermal product curves obtained from both CFD and experimental data with vary-

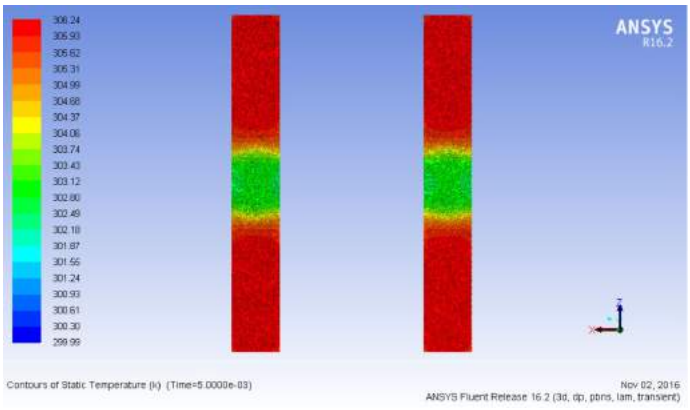

(a) 0.01% of water in oil

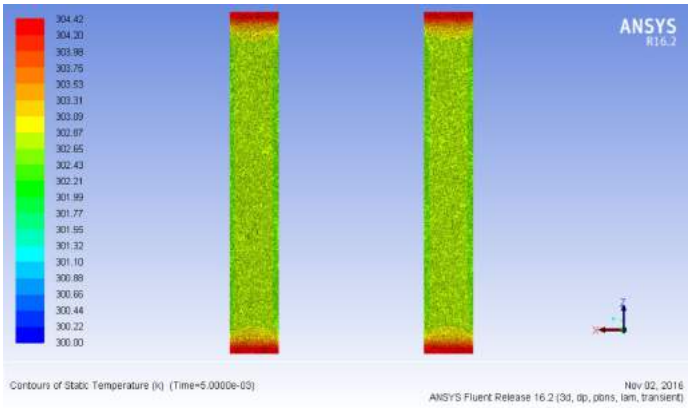

(b) 1% of water in oil

FIGURE 8: Contour plots of Temperature for water in oil

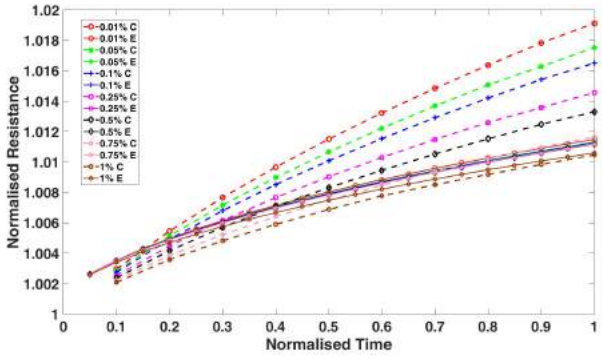

(a) Thermal product curves for water in acetone

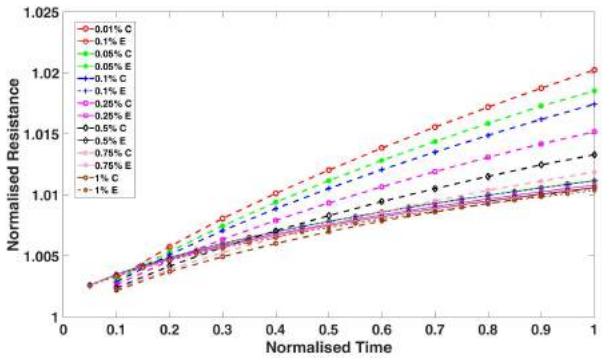

(b) Thermal product curves for water in oil

ing concentrations of water in acetone and oil. One can note that the agreement for 0.75 and 1% is quite good whereas, for lower concentrations the agreement is not so good. Also it can be noted that the initial part of the curves don't agree quite well with each other similar to that observed for without contamination cases. This trend is observed for both water in acetone and water in oil.

Table 3 shows the comparison of the final values from both experimental and CFD data. We see that the agreement is quite good for higher concentrations although for lower concentrations it is quite bad. One of the possible reasons for some of the disagreements seen between CFD and experiments could be the difficulty of placing small concentrations of the contaminant (i.e. water drop) in experiments (for example a 2 μL corresponding to 0.01% by mass) exactly on the sensor in both acetone and oil. A second reason might be the inadequacy of the conjugate heat transfer model itself, where it tends to over-predict the temperature and finally the nodes for solid and fluid interfaces were not merged exactly as exact merging requires the use of pinching operation. However, with pinching the number of cells with very high skewness and aspect ratio increases and can lead to instabil-

Water in Acetone			
Concentration	Computation	Experiment	% Difference
0.01%	1.019	1.0115	0.74
0.05%	1.018	1.0113	0.66
0.1%	1.017	1.0112	0.57
0.25%	1.015	1.011	0.4
0.5%	1.013	1.0108	0.22
0.75%	1.011	1.0105	0.05
1%	1.0106	1.01	0.04
Water in Oil			
0.01%	1.02	1.0115	0.84
0.05%	1.019	1.0113	0.76
0.1%	1.017	1.0112	0.57
0.25%	1.015	1.0108	0.42
0.5%	1.013	1.0106	0.24
0.75%	1.012	1.0105	0.15
1%	1.011	1.01	0.1

TABLE 3: Comparison of final values of thermal product (resistance) between computations and experiments

ity. Hence, rather than pinching, proper face sizing and inflation was done at the interface to ensure smooth transition of mesh from solid to fluid.

Conclusions

A new sensor to detect oil contamination and condition has been developed and tested for various cases of liquid contamination. Both numerical and experimental data show good agreement with each other for both with and without contamination. A thorough understanding of the heat transfer mechanism is understood which will help in further development of the sensor. The good agreement also suggests that the numerical model used is sufficient to capture all the details although for lower concentrations, it might be beneficial to look at different modelling techniques.

REFERENCES

[1] C.Chaiyachit, S.Satthamsakul, W.Sriratana, and T.Suesut, 2012. "Hall effect sensor for measuring metal particles in lubricant". In Proceeding of the Internation MultiConference of Engineers and Computer Scientists.

[2] Herrmann, F., Jakoby, B., Rabe, J., and Buttgenbach, S., 2001. *Microacoustic Sensors for Liquid Monitoring*, Vol. 9. Wiley VCH.

[3] Hammond, J., Lec, R., Zhang, X., D.G.Libby, and Prager, L., 1997. "An acoustic automotive engine oil quality sensor". In IEEE International, Frequency Control Symposium.

[4] Sridhar, V., and Chana, K. S., 2016. "A novel sensor for detection of oil condition and contamination based on a thermal approach". In 12th International Conference on Heat Transfer, Fluid Mechanics and Thermodynamics.

[5] Schultz, D., and Jones, T., 1973. Heat-transfer measurements in short-duration hypersonic facilities. Tech. Rep. AGARD165, University of Oxford, February.